Magnetospatial dispersion effect in magnetic semiconductors $Cd_{1-x}Mn_xTe$

B. B. Krichevtsov, R. V. Pisarev, A. A. Rzhevsky, and V. N. Gridnev
A. F. Ioffe Physico-Technical Institute of the Russian Academy of Sciences, St. Petersburg 194021, Russia

H.-J. Weber
Physics Department, Dortmund University, 44221 Dortmund, Germany
(Received 25 August 1997)

We show that a magnetic field induces a strong birefringence in noncentrosymmetric cubic crystals of $Cd_{1-x}Mn_xTe$ in the Voigt configuration $\mathbf{k}\perp\mathbf{B}$. The induced birefringence can be separated into the linear magnetospatial dispersion birefringence of a kB type, and the quadratic Voigt birefringence of B^2 type. The kB effect is strikingly anisotropic, whereas the B^2 effect is fully isotropic. A microscopic theory is proposed for explaining the dispersion of symmetric and antisymmetric contributions to the kB birefringence near the absorption band edge. [S0163-1829(98)04119-8]

A large variety of magneto-optical (MO) and spatial dispersion (SD) optical phenomena can be described in the most general form by a series expansion of the optical dielectric tensor ϵ_{ij} as a function of the magnetic field $\mathbf{B}$ and the wave vector of light $\mathbf{k}$:[1,2]

$$\epsilon_{ij}(\omega,\mathbf{k},\mathbf{B})=\epsilon_{ji}(\omega,-\mathbf{k},-\mathbf{B})=\epsilon_{ij}(\omega)+\alpha_{ijk}B_k+\beta_{ijkl}B_kB_l+\delta_{ijk}k_k+\eta_{ijkl}k_kk_l. \quad (1)$$

The best known examples represented by different terms in Eq. (1) are the Faraday rotation (FR) $\sim B$, the Voigt birefringence (VB) $\sim B^2$, the optical activity $\sim k$, and the Lorentz birefringence $\sim k^2$. These effects have been studied in a large number of materials and the underlying microscopic mechanisms are quite well understood.

In contrast, much less attention has been paid to the magnetic-field-induced SD effects, which are bilinear in the wave vector of light $\mathbf{k}$ and the applied magnetic field $\mathbf{B}$ (kB effects):[1,2]

$$\Delta\epsilon_{ij}(\omega,\mathbf{k},\mathbf{B})=\gamma_{ijkl}B_kk_l, \quad (2)$$

where $\hat{\gamma}$ is the axial fourth-rank tensor allowed in all noncentrosymmetric crystals. It is evident that a study of relevant optical phenomena can provide information on the electronic structure of solids that cannot be gained from studies of optical phenomena due to material tensors in Eq. (1). Examples of experimental manifestations of kB-type contributions to optical phenomena are scarce and restricted to the alteration of the optic absorption spectrum in the region of exciton transitions when the magnetic field is reversed,[3,4] the magnetic-field-induced ellipticity[5] and the magnetic birefringence in the transparency region.[6,7] Being due to the higher-order perturbations of the electronic structure, effects of the kB type are much smaller than the linear MO effects. Additional experimental difficulties for their observation arise because in the longitudinal Faraday configuration they are masked by the much stronger Faraday effect, whereas in the transverse Voigt configuration they overlap with B^2 and k^2 effects.

All data thus far reported were obtained in diamagnetic crystals, in which linear MO effects are small, and hence, kB effects have to be very small. Larger kB effects might be expected in magnetic semiconductors possessing huge Faraday rotation[8–10] and Voigt birefringence.[11] In this paper we report results on magnetic-field-induced birefringence of linearly polarized light in diluted magnetic semiconductors $Cd_{1-x}Mn_xTe$. We used an experimental technique that allowed us to avoid the Faraday rotation contribution to the observed signals and an unambiguous separation of the induced birefringence into kB and B^2 contributions. We prove that the magnitude of the kB effect increases linearly with the concentration of magnetic Mn^{2+} ions. We show that the new MO effect of kB type shows a dispersion different from that of Faraday rotation and Voigt birefringence. We developed a microscopic theory and its predictions are in good agreement with the experiment.

Equation (2) can be written in a form containing a symmetric and an antisymmetric contributions to the kB effect

$$\Delta\epsilon_{ij}=\gamma^S_{ijkl}B_kk_l+g_{ijs}[\mathbf{B}\cdot\mathbf{k}]_s. \quad (3)$$

$Cd_{1-x}Mn_xTe$ crystals belong to the cubic class T_d, in which the tensor $\hat{\gamma}^S$ is symmetric under the permutation of the first and last two indices and has one independent component $\gamma_{xxyy}=\gamma_{yyzz}=\gamma_{zzxx}=-\gamma_{yyxx}=-\gamma_{zzyy}=-\gamma_{xxzz}=A$. The tensor $\hat{g}$ is fully symmetric and has only one independent component $g_{xyz}=g$. In the Voigt geometry $\mathbf{k}\perp\mathbf{B}$ the magnetic birefringence is defined by tensors $\hat{\gamma}$ and $\hat{\beta}$ from Eqs. (2) and (1). For $\mathbf{k}\|[110]$ and $\mathbf{B}\|[001]$, the two axes of the optical indicatrix due to the tensor $\hat{\gamma}$ are in the (110) plane at $\pm 45°$ with respect to the direction of $\mathbf{B}$ and the relevant birefringence is

$$\Delta n=gBk/n, \quad (4)$$

where $n=\sqrt{\epsilon_0}$ is the index of refraction. For $\mathbf{B}\|[1\bar{1}0]$, the two axes are along the $[1\bar{1}0]$ and $[001]$ axes and

$$\Delta n=(3A+2g)Bk/4n. \quad (5)$$

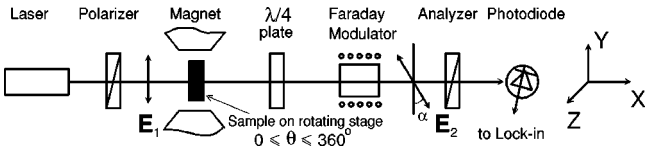

FIG. 1. Schematic diagram of the experimental setup.

The second contribution to the magnetic linear birefringence stems from the tensor $\hat{\beta}$ in Eq. (1):

$$\Delta n(\Theta,B)\sim f(\Theta)B^2/2n, \tag{6}$$

where Θ denotes the orientation of **B** in the (110) plane with respect to the [001] axis. Thus the kB and B^2 contributions overlap and the experimental method should provide a possibility to separate them.

The experimental setup is shown in Fig. 1. A laser beam (He-Ne laser, $\lambda=0.633$ μm and 1.15 μm, and Al_2O_3:Ti laser, $\lambda=0.7-0.83$ μm) passes through a polarizer, a sample in the gap of an electromagnet, a quarter wave $\lambda/4$ plate, a Faraday type MO modulator, and an analyzer. An important expedient that allowed measuring the anisotropy of magnetic birefringence was to place the sample on a stage that could be rotated by 360° around the laser beam axis. The transmitted light was detected by a photodiode and the signal was measured using a lock-in amplifier. The sensitivity of measuring the induced rotation $\alpha=(\pi l/\lambda)\Delta n$ was 10″. The magnetic field range was ± 1.5 T. All measurements were performed at $T=294$ K. The plane-parallel (110) and (111) samples with a thickness l of 0.6–1.5 mm were prepared from $Cd_{1-x}Mn_xTe$ single crystals ($x=0,0.25,0.35,0.42,0.52$).

Two polarization configurations were used. In case (a) the incident linear polarization $\mathbf{E}_1$ was parallel to the magnetic field **B** (**E**$\|$**B**), while in case (b) it was at 45° to **B** (**E**45°**B**). In case (a), the B^2 contribution vanishes and only the kB contribution is measured. In case (b), the two contributions are measured simultaneously. The Faraday rotation in $Cd_{1-x}Mn_xTe$ crystals is about three orders of magnitude larger than the kB effect and hence can easily meddle into observed signals when **k** and **B** are not perfectly perpendicular. To prevent this meddling the control measurements and alignments were taken without the $\lambda/4$ plate. The absence of any rotation was taken as a proof of exact 90° alignment of **k** and **B** vectors.

As an example we display in Fig. 2 the induced birefringence as a function of magnetic field at $\lambda=0.633$ μm in the (110) sample ($x=0.42$) for two polarization geometries. The different sets of data correspond to different azimuthal positions of the sample. In case (a) the birefringence is a linear odd function of magnetic field, thus unambiguously proving the presence of the kB effect solely. In case (b), the birefringence is essentially asymmetric upon field reversal due to the simultaneous presence of kB and B^2 contributions. The quadratic Voigt birefringence was found to be isotropic.

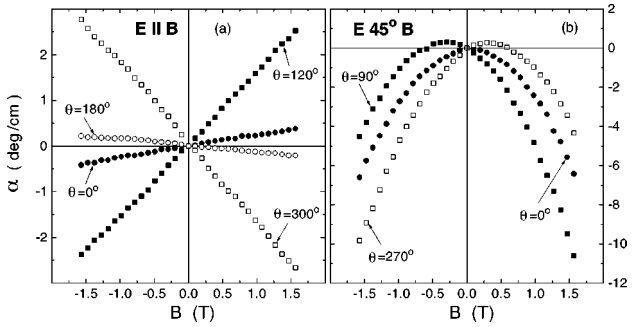

FIG. 2. Magnetic linear birefringence in the (110) sample of $Cd_{1-x}Mn_xTe$ ($x=0.42$) for two polarization geometries $\mathbf{E}_1\|\mathbf{B}$ (a) and $\mathbf{E}_1$ at 45° to **B** (b).

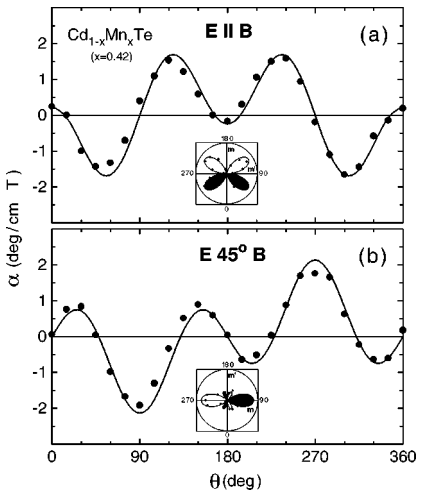

FIG. 3. Rotational anisotropy of the magnetic linear birefringence of kB type in a (110) sample of $Cd_{1-x}Mn_xTe$ ($x=0.42$). Solid curves are best fit calculations. The insets show the same data presented in polar plots.

Figure 3 shows the rotational anisotropy of the kB effect. In case (a) the effect reverses sign when $\mathbf{B}\rightarrow-\mathbf{B}$, when $\Theta\rightarrow\Theta+180°$, and when the sample is rotated by 180° around the laboratory Z axis. However, it remains unchanged by the 180° rotation around the Y axis. In case (b) the kB birefringence reverses sign when the sample is rotated by 180° around the Y axis, however, it remains unchanged by rotation around the Z axis. All these features are in perfect agreement with the symmetry predictions. Depending on the polarization geometry the rotational anisotropy can be described in the (110) plane by two contributions proportional to $\cos\Theta$ ($\sin\Theta$) and $\cos3\Theta$ ($\sin3\Theta$). In (111) samples the kB effect exhibits an anisotropy proportional to a $\cos3\Theta$ ($\sin3\Theta$) function.

Figure 4(a) shows the normalized components of the symmetric A/x and antisymmetric g/x contributions calculated from the spectral variations of the kB effect in geometries $\mathbf{E}\|\mathbf{B}$ and **E**45°**B** in four $Cd_{1-x}Mn_xTe$ samples as a function of (E_g-E), where E_g is the energy gap calculated using Eq. (4a) from Ref. 8 and E is the photon energy. The inset shows the concentration dependence of the specific rotation α due to the kB effect measured in geometry **E**45°**B** ($\Theta=270°$, see Fig. 3) at $E_g-E=0.45$ eV. Linear dependence $\alpha(x)$ and the fact that the magnitude of the kB effect in CdTe is at least an order of magnitude smaller than in Mn-containing crystals proves that the origin of the kB effect is related to Mn^{2+} ions. Figure 4(b) shows the data for normalized Faraday rotation R_F/x and quadratic Voigt birefringence B_V/x^2 measured in the same samples. Figures 4(a) and 4(b) demonstrate the universal behavior of the kB effect, R_F, and B_V

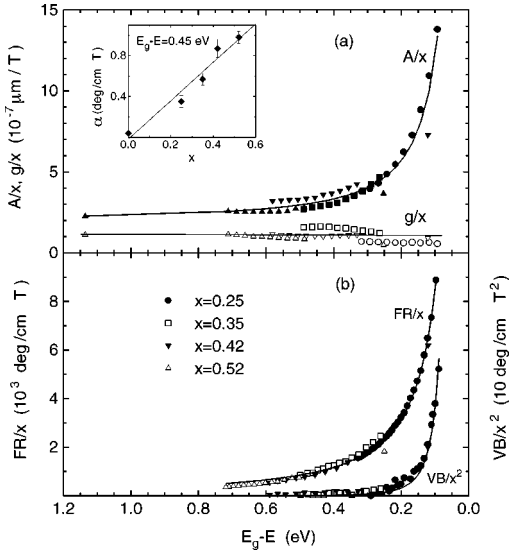

FIG. 4. Dispersion of normalized components of symmetric A/x and antisymmetric g/x contributions to the kB effect, Faraday rotation R_F/x and Voigt birefringence B_V/x^2 in four $Cd_{1-x}Mn_xTe$ crystals.

and provide a unique opportunity to compare both the absolute values and the energy dispersions of three different MO effects in four samples. The Faraday rotation is about three orders of magnitude larger than the kB effect. Near the band gap the kB and B^2 effects are of comparable magnitudes at a field of about 1 T. Note that the value $A/x=10^{-6}$ μm/T corresponds approximately to the rotation $\alpha/x=6$ deg/cm T.

The dispersion of three MO effects in different samples can be well fitted by a function $d+t(E_g-E)^{-\tau}$ shown by solid lines in Fig. 4, where $\tau\approx1.4$ for the normalized component of symmetric tensor A/x, $\tau\approx1.5$ for the R_F/x, and $\tau\approx3.5$ for the B_V/x^2. The antisymmetric component g/x does not show any resonant behavior near the band gap ($t=0$). The frequency-independent part $d=0$ for R_F and B_V. In contrast $d\approx2\times10^{-7}$ μm/T for A/x and $d\approx1\times10^{-7}$ μm/T for g/x.

The previously published theoretical works concerning the kB effect have concentrated on the excitonic mechanism[5,7] or intraband transitions[12] and thus cannot be applied to our data. We present a semiquantitative consideration that takes into account interband transitions from the valence band Γ_8 to the conduction band Γ_6. Taking the derivative of the optical tensor $\epsilon_{ij}(\omega,\mathbf{k},\mathbf{B})$ (Ref. 13) with respect to k_l and B_k and retaining only the most important near the band edge ''resonance'' term, we get

$$\gamma_{ijkl}=\frac{4\pi\hbar^2}{E^2V}\frac{\partial}{\partial k_l\partial B_k}\sum_{r,s,\mathbf{q}}\frac{J^i_{s\mathbf{q},r\mathbf{q}-\mathbf{k}}(-\mathbf{k})J^j_{r\mathbf{q}-\mathbf{k},s\mathbf{q}}(\mathbf{k})}{E_{r\mathbf{q}-\mathbf{k}}-E_{s\mathbf{q}}-E}\Bigg|_{\mathbf{k},\mathbf{B}\to0}, \tag{7}$$

where V is the crystal volume; $r=\pm1$ and $s=\pm1$, ±3 enumerate the conduction and valence band states, respectively; $\mathbf{J}(\mathbf{k})$ is the Fourier transform of the current operator. We shall analyze the most singular contributions to γ_{ijkl} near the band edge. For this reason we neglect the dependence of the current matrix element on magnetic field because the corresponding term slowly varies with frequency. We shall differentiate only the energy denominator with respect to B_k. In doing this we shall use the dependence of $E_{r\mathbf{q}-\mathbf{k}}$ and $E_{s\mathbf{k}}$ on $\mathbf{B}$ for the limiting case when $\mathbf{B}$ is small. It produces the anisotropic splittings[9] $\Delta E_{\rm lh}(\mathbf{q},\mathbf{B})=\pm b\sqrt{4-3\cos^2\theta}$ and $\Delta E_{\rm hh}(\mathbf{q},\mathbf{B})=\pm3b\cos\theta$ of light- and heavy-hole bands, respectively, and the isotropic splitting $\Delta E_c(\mathbf{q},\mathbf{B})=\pm3a$ of the conduction band. θ is the angle between the wave vector $\mathbf{q}$ and the magnetization $\mathbf{M}$ of the Mn^{2+} ions. a and b are proportional to the magnetization M and describe the exchange interaction of the Mn^{2+} ions with band electrons.[9]

The kB effect is due to a combined action of the inversion asymmetry of the crystal and the magnetic field and, hence, should be proportional to an inversion asymmetry parameter. There exist several such parameters for the zinc-blende structure[14] that enter the interband current operator $\mathbf{J}(\mathbf{k})$ or determine the spin splittings of the conduction and valence bands.

For the calculation of $\mathbf{J}(\mathbf{k})=(e/2)(\mathbf{v}e^{-i\mathbf{k}\cdot\mathbf{r}}+e^{-i\mathbf{k}\cdot\mathbf{r}}\mathbf{v})$, where $\mathbf{v}=(1/\hbar)\partial H_{cv}/\partial\mathbf{q}$ is the velocity operator, we use the interband effective Hamiltonian

$$H_{cv}=\sqrt{3}[P(\mathbf{q}\cdot\mathbf{R})+iBs_{inm}q_iq_nR_m], \tag{8}$$

where $\mathbf{R}$ is the operator of a polar vector in the basis Ψ_{Γ_6}, Ψ_{Γ_8}, s_{inm} is a fully symmetric tensor, P and B are the Kane parameters, the latter being due to the inversion asymmetry. We have also analyzed contribution to γ_{ijkl} proportional to the inversion asymmetry parameter δ_0, which enters the derivative $\partial E_{r\mathbf{q}}/\partial\mathbf{q}=\hbar^2\mathbf{q}/m_c+r\delta_0\mathbf{f}(\mathbf{q})$, where $\mathbf{f}$ is a quadratic function of $\mathbf{q}$, as well as the contribution due to the parameter C_0 defining the linear in $\mathbf{q}$ spin-orbit splitting of the valence band and entering Eq. (7) through the wave functions $\psi_{s\mathbf{q}}$.

Integration in Eq. (7) leads to a cumbersome expression for A and to $g=0$. The zero result for g is in agreement with our experimental data, which show a frequency-independent behavior of g and its smallness in comparison with A, especially near the band gap. The frequency dependence of the contributions to A from each of the parameters B, δ_0, and C_0 near the band gap has the form $A\sim(E_g-E)^{-1/2}$. The discrimination between various contributions remains an unsolved problem and requires a more elaborate theory.

The frequency behavior of A calculated in terms of this approach is not strong enough to explain the experimental data. This is quite similar to what is encountered in the interpretation of the Faraday rotation data.[10] The Faraday rotation near the band gap should vary faster, if one takes into account a wave-vector dependence of the exchange interaction parameters a and b of band electrons with Mn^{2+} ions. The degree of this enhancement depends on the extent q_0 of a region in the Brillouin zone near the Γ point in which these parameters do not decrease appreciably. If we take the limit $q_0\to0$, then we obtain the frequency dependence

$$A=t(E_g-E)^{-3/2}+d(E), \tag{9}$$

where $d(E)$ is a slowly varying function of photon energy due to the terms omitted in our calculations. This dependence is in good agreement with experiment.

In conclusion, we have shown that the magnetic field induces strong linear birefringence in cubic crystals of magnetic semiconductors $Cd_{1-x}Mn_xTe$ in the Voigt configuration $\mathbf{k} \perp \mathbf{B}$. The data obtained allow an unambiguous separation of the induced birefringence into two contributions. The first of kB type is due to the magnetospatial dispersion effects and reveals a striking anisotropy. The Voigt birefringence of B^2 type is fully isotropic. We measured in the same samples the Faraday rotation, which provided us with a unique opportunity to compare the absolute values and energy dispersion of three different MO effects. The comparison convincingly proves their different microscopic origins, though their enhancement in all cases is due to a strong exchange interaction of Mn^{2+} ions with band carriers. Further studies of magnetic birefringence can provide new information on the splitting of electronic transitions due to the inversion asymmetry. We anticipate a strong increase of magnetic birefringence in magnetic semiconductors at low temperatures, as usually occurs with the Faraday rotation and Voigt birefringence. Our measurements of the kB effect in CdTe show that it can be measurable in nonmagnetic semiconductors as well.

This research was supported by the INTAS, the DFG, the RFBR, and the Program Fundamental Spectroscopy.

[1] V. M. Agranovich and V. L. Ginzburg, *Spatial Dispersion in Crystal Optics and the Theory of Excitons*, 2nd ed. (Springer-Verlag, Berlin, 1984).

[2] D. L. Portigal and E. Burstein, J. Phys. Chem. Solids **32**, 603 (1971).

[3] J. J. Hopfield and D. G. Thomas Phys. Rev. Lett. **4**, 357 (1960).

[4] E. F. Gross, B. P. Zacharchenya, and O. V. Konstantinov, Fiz. Tverd. Tela (Leningrad) **3**, 305 (1961).

[5] E. L. Ivchenko, V. P. Kochereshko, G. V. Mikhailov, and I. N. Uraltsev, Pis'ma Zh. Eksp. Teor. Fiz **37**, 137 (1983); Phys. Status Solidi B **121**, 221 (1984).

[6] V. A. Markelov, M. A. Novikov, and A. A. Turkin, JETP Lett. **25**, 378 (1977).

[7] O. V. Gogolin, V. A. Tsvetkov, and E. G. Tsitsichvili, Zh. Eksp. Teor. Fiz. **87**, 1038 (1984).

[8] J. K. Furdyna, J. Appl. Phys. **65**, R29 (1988).

[9] J. A. Gaj, in *Semiconductors and Semimetals*, edited by J. K. Furdyna and J. Kossut (Academic Press, Boston, 1988), Vol. 25, p. 275.

[10] S. Hugonnard-Bruyère, C. Buss, F. Vouilloz, R. Frey, and C. Flytzanis, Phys. Rev. B **50**, 2200 (1994).

[11] Eunsoon Oh, D. U. Bartholomew, A. K. Ramdas, J. K. Furdyna, and U. Debska, Phys. Rev. B **44**, 10 551 (1991).

[12] Y.-F. Chen, M. Dobrowolska, J. K. Furdyna, and S. Rodriguez, Phys. Rev. B **32**, 890 (1985).

[13] G. Bir and G. Pikus, *Symmetry and Strain-Induced Effects in Semiconductors* (Wiley, New York, 1974).

[14] E. Kane, in *Physics of III-V Compounds*, edited by R. Willardson and A. Beer, *Semiconductors and Semimetals* Vol. 1 (Academic Press, New York, 1966), p. 75.